GEOLOGICA BELGICA (2010) 13/3: 183-196

RIETVELD REFINEMENT STRATEGY FOR QUANTITATIVE PHASE ANALYSIS OF PARTIALLY AMORPHOUS ZEOLITIZED TUFFACEOUS ROCKS

Ruben SNELLINGS*, Lieven MACHIELS, Gilles MERTENS & Jan ELSEN

(8 figures and 3 tables)

Department of Earth and Environmental Sciences, K.U.Leuven, Celestijnenlaan 200E, B-3001 Heverlee, Belgium. E-mail: ruben.snellings@ees.kuleuven.be
**corresponding author*

ABSTRACT The Rietveld method has become one of the most popular methods in quantitative mineralogical analysis based on X-ray powder diffraction. An estimate of the amorphous phase content can be made by introducing a known amount of an appropriate internal standard. This method was applied to a selected set of zeolitized tuffaceous rocks to develop guidelines for Rietveld quantitative phase analysis in complex mixtures. A local sensitivity analysis of selected refinable parameters was performed and phase abundance results for synchrotron and laboratory based X-ray diffraction data collection were compared. The calculated amorphous phase fraction showed a very high sensitivity towards the refined amount of internal standard, in particular when small amounts of amorphous phase were encountered in the samples. Optimal reproducibility of phase abundance results was obtained when a sufficient number of background polynomials was employed and the internal standard thermal parameters were not refined. A very good correlation between laboratory and synchrotron data was achieved when the communicated refinement strategy was followed, supporting the use of laboratory equipment for routine quantitative mineralogical analysis.

KEYWORDS. natural zeolites, Rietveld method, quantitative analysis, tuffs, amorphous phase, synchrotron

1. Introduction

During the last half century X-ray powder diffraction (XRPD) has become one of the most appropriate and proliferous techniques for the quantification of mineral abundances in natural and industrial polycrystalline materials. XRPD offers significant advantages in processing speed and simplicity over other traditional methods of quantitative mineralogical analysis such as point-counting on thin sections or inference from bulk chemistry (Bish & Post, 1993). Especially when applied to fine-grained materials not suited for optical examination, such as clay-rich sediments or zeolitized volcanogenic rocks, or to large scale quality control on industrial materials, e.g. cements (Scarlett *et al.*, 2001) and ceramics, the advantages of XRPD-based methods become clear. The recent advent of rapid and effective detector systems, conjointly with the increasing computational abilities of hardware and quantification software, drastically shortened data collection and processing times, allowing accurate and precise on-line monitoring of phase content in well calibrated systems (Gualtieri & Brignoli, 2004).

A simultaneous evolution in the methodology of extracting information from XRPD patterns is noted by the rise of full-pattern fitting methodologies. Previously, quantification methods were based on the comparison of single or sets of reflection peak intensities or integrated peak areas with an added internal standard or with standard patterns (e.g. Klug & Alexander, 1974). Several problems affected the quantification process, most significantly peak overlap, problems related to sample preparation such as particle statistics and preferred orientation effects of the crystallites and problems related to the selection of appropriate standards (Hill & Howard, 1987).

The approach taken in full-pattern fitting methods is to make use of the information contained in the entire diffraction pattern and allows the inclusion of areas subject to strong peak overlapping into the quantification procedure. Furthermore, consideration of the complete pattern mitigates the effects of preferred orientation and primary extinction. The refinement procedure is based on the minimization of the weighted, squared differences between the observed and calculated intensities at every step in the diffraction pattern. In general, full-pattern fitting methods can be subdivided into two different approaches. On the one hand, profile summation methods that involve the collection of XRPD patterns of a broad set of standards which are subsequently fitted by weighted summation over the whole pattern to the observed pattern (e.g. Środoń *et al.*, 2001; Eberl, 2003). On the other hand, in the Rietveld method the diffraction profile is calculated using crystal structure information, peak shape functions reflecting instrumental and microstructural parameters and a background contribution.

Though both profile summation and Rietveld methods perform equally well in quantitative analysis (Madsen *et al.*, 2001), unlike profile summation methods the Rietveld

method does not require a time-consuming calibration with a broad set of appropriate standard materials. However, the crystal structures of all crystalline phases need to be known approximately. The possibility of refining crystal structural parameters such as unit cell parameters, site fractional coordinates, occupancy and thermal factors permits a wealth of additional information to be extracted from the powder diffraction pattern (McCusker *et al.*, 1999).

In the Rietveld method, the difference between all data set points of the observed and the calculated profiles is minimized by a least squares refinement of selected parameters. The progress of the refinement is monitored by a number of agreement indices, among those commonly used are the weighted profile R_{wp} index and the 'goodness of fit' (S) index which is the ratio of R_{wp} over the statistically expected R_{exp}. R_{wp} and R_{exp} are defined as

$$R_{wp} = \left(\sum_i w_i \left(y_{i,obs} - y_{i,calc} \right)^2 / \sum_i w_i \left(y_{i,obs} \right)^2 \right)^{1/2} \quad (1)$$

$$R_{exp} = \left((N - P) / \sum_i w_i \left(y_{i,obs} \right)^2 \right)^{1/2} \quad (2)$$

where $y_{i,obs}$ is the observed intensity, $y_{i,calc}$ the calculated intensity and w_i the weight at point i in the diffraction profile, N is the number of observations and P the number of parameters. For more theoretical details regarding the Rietveld method, the reader is referred to the literature (Rietveld, 1969; Young 1993).

Originally conceived as a method for structure refinement by neutron diffraction, the method was subsequently suited to quantitative mineralogical analysis using X-ray diffraction (Bish & Howard, 1988; Hill, 1991, Bish and Post, 1993). The calculated profile yields scaling factors for each phase to fit the intensity of the observed pattern. These scale factors are related to the respective relative weight fractions by equation (3) (Hill & Howard, 1987):

$$W_i = \frac{S_i (ZMV)_i}{\sum_{j=1}^{n} S_j (ZMV)_j} \quad (3)$$

where W_i and S_i represent the weight fraction and the refined scale factor of phase i, ZMV identifies with the phase specific parameters Z, the number of formula units per unit cell, M, the mass of the formula unit, and V, the volume of the unit cell. It should be noted that both M and V are variable when site occupancies and unit cell parameters are allowed to refine. If amorphous or unidentified phases exist in the mixture, the normalization condition in equation (3) results in overestimated weight fractions. Therefore a known amount of crystalline internal standard can be introduced and weight fractions can be rescaled as in equation (4):

$$W_{i,c} = W_i \frac{W_{s,w}}{W_s} \left(\frac{1}{1 - W_{s,w}} \right) \quad (4)$$

where $W_{i,c}$ is the recalculated actual weight fraction of phase i, W_i and W_s are the refined weight fractions of phase i and the internal standard respectively, and $W_{s,w}$ is the actual added weight of the internal standard. The weight fraction W_a pertaining to X-ray amorphous or non-identified phases is then calculated as $W_a = 1 - \sum_i W_{i,c}$. An accurate assessment of the amorphous phase content is very important to obtain correct absolute weight fractions. Ideally an internal standard of known crystallinity and of micronized grain size and/or absorption coefficient similar to the sample mixture should be employed (*cf.* Brindley correction; Brindley, 1945; Taylor & Matsulis, 1991; De la Torre *et al.*, 2001).

Due to its versatility the Rietveld quantification method is finding widespread application in the mineral industry. Especially accuracy and detection limits in complex polycrystalline mixtures benefit strongly (Bish & Post, 1993; Gualtieri, 2000; Scarlett et al., 2001; Pritula *et al.*, 2004; Walenta & Füllmann, 2004; Mitchell *et al.*, 2006; Gualtieri *et al.*, 2006).

Quantification of the mineral content in zeolitized tuffaceous rocks is useful to investigate the zeolitisation processes during diagenesis and low-grade metamorphism and to assess the exploitability of deposits for industrial purposes (Gualtieri, 1996). In general, zeolite deposits show a relatively large variability in terms of zeolite crystal chemistry, zeolite content and amorphous phase content due to locally heterogeneous zeolite formation conditions (e.g. Weisenberger & Spürgin, 2009). It is then obvious that the basic assumption for Rietveld refinement of known crystal structures is not completely fulfilled. Exchangeable cation and zeolite water content can exert an important bias on the refined weight fractions by changing the average site occupancies and positions of extraframework species and simultaneously affecting the unit cell weight. Furthermore, the presence of variable amounts of the zeolite parent material, i.e. amorphous volcanic glass, or semi-crystalline alteration products introduces an additional source of inaccuracy. The importance of the quantification of this amorphous phase is important for industrial applications since it can alter the physical properties of the material significantly (e.g. Suherman *et al.*, 2002; De la Torre *et al.*, 2001; Gualtieri, 2000).

In this paper, the influence of the most important systematic errors in Rietveld quantitative analysis will be discussed with regard to their application on natural zeolitized materials. A set of zeolitized tuffs originating from geologically different areas was selected for experimentation. The sensitivity of the abundances of the zeolite and amorphous phases towards refinement of the zeolite crystal structure, the background, the atomic isotropic displacement parameters of the internal standard and preferred orientation corrections were evaluated.

Additionally, data collection regimes were evaluated by using two differing X-ray sources and sample loading techniques: laboratory-based CuK$\alpha_{1,2}$ radiation with back-loading in Bragg-Brentano reflection mode, and synchrotron radiation of 0.49725 Å wavelength on capillaries in transmission mode. The aim is to propose guidelines for Rietveld quantitative mineralogical analysis in complex mixtures containing chemically variable crystalline phases together with amorphous phases.

2. Experimental methods

2.1. Materials

The selection of starting materials was based on a preliminary identification of sample mineralogy. All investigated samples are natural zeolitized tuffs, ranging in zeolite content from approximately 50 to 95 wt% and in amorphous content from 4 to 45 wt%. The zeolitized tuffs selected for this study consist mainly of clinoptilolite and/or mordenite type zeolite minerals. The samples additionally contain varying amounts of accessory phases and amorphous material. Silica polymorphs, such as quartz and opal CT (intercalations of cristobalite and tridymite), plagioclase, K-feldspars and smectite were encountered. References to the origin and the chemical and mineralogical composition of the samples are enlisted in Table 1. Weakly crystalline phases such as Opal CT and authigenous smectite were included in the amorphous phase fraction. The presented mineralogical quantification results were obtained following the recommendations further elaborated in the Results section. Bulk chemical analyses were performed using an anhydrous lithium metaborate fusion flux to dissolve the samples, the obtained solutions were analysed with inductively coupled plasma optical emission spectrometry (ICP-OES). Loss on ignition (LOI) was determined after heating the samples for 2 h at 1050 °C.

Sample preparation for quantitative analysis was procured following the procedure outlined by Środoń *et al*. (2001). The preparation consisted of preliminary grinding of the samples to grain sizes below 400 μm and wet milling in methanol of the crushed sample intermixed with a 10 wt% ZnO internal standard in a McCrone Micronising Mill to obtain a narrow grain size distribution below 20 μm. The resulting slurries were evaporated and subsequently finely dispersed by grinding in an agate mortar. Despite the larger difference in absorption coefficient with the sample mixture, ZnO (Baker) was preferred over corundum as internal standard because of stronger reflections and apparent absence of X-ray amorphous material. The very small ZnO particle size of approximately 1 μm (Środoń *et al*., 2001) renders microabsorption effects insignificant.

Zeolites show reversible water absorption characteristics in function of the atmospheric relative

Table 1. Overview of starting materials selected for quantitative mineralogical analysis. Both chemical composition and the final mineralogical composition (esd in parentheses) are presented. Rietveld quantitative phase analysis was performed according to the guidelines specified in this paper, i.e. using literature internal standard thermal parameters, 15 Chebyshev background polynomials, and refined zeolite structures for samples A, B, C, E and G. Following references describe the deposit geology: [a] Barker *et al*. (2004), [b] Eyde (1982), [c] Gude & Sheppard (1988), [d] Flood & Taylor (1991), [e] Honrado *et al*. (2009), [f] Benito *et al*. (1998).

	A	B	C	D	E	F	G
	Winston,	Bowie,	Buckhorn,	Castle Mountain,	Mangatarem,	Mangatarem,	Cabo de Gata,
	New Mexico,	Arizona,	New Mexico,	New South Wales,	Luzon,	Luzon,	Almeria,
Occurrence	USA[a]	USA[b]	USA[c]	Australia[d]	Philippines[e]	Philippines[e]	Spain[f]
Chemistry (wt%)							
Al_2O_3	11.83	12.40	12.26	12.13	10.56	11.53	11.45
SiO_2	67.30	65.24	65.26	71.43	65.88	55.19	68.32
CaO	3.21	3.75	3.42	2.76	3.36	2.84	1.36
MgO	1.18	1.21	1.51	0.90	0.14	2.49	0.86
K_2O	2.73	1.24	1.30	1.04	0.54	0.42	1.55
Na_2O	0.78	1.27	2.01	1.91	1.89	0.42	3.03
Fe_2O_3	1.30	0.88	1.48	1.23	1.42	4.83	1.20
TiO_2	0.23	0.13	0.17	0.20	0.39	0.61	0.10
LOI	12.04	13.65	12.31	8.94	14.92	19.25	11.57
SUM	100.61	99.77	99.71	100.54	99.10	97.58	99.46
Mineralogy (wt%)							
Clinoptilolite	71.7 (3)	69.8 (2)	93.4 (2)	30.9 (3)		43.5 (4)	
Mordenite				17.0 (3)	72.6 (2)	11.8 (5)	52.4 (4)
Quartz	8.6 (1)		1.4 (1)	23.9 (2)	0.5 (1)	1.1 (1)	1.4 (1)
K-feldspar	13.1 (4)						5.6 (2)
Plagioclase				7.7 (2)			4.8 (2)
Amorphous	6.6 (8)	30.2 (9)	5.2 (11)	20.7 (8)	26.9 (9)	43.6 (10)	33.6 (9)

humidity. This variation can lead to percent changes in absolute weight. Due to the elevated sensitivity of the amorphous phase fraction to the ratio of the actual over the refined weight fraction of the internal standard, it is therefore advisable to determine the actual weight fraction of internal standard accurately and minimize the variation in zeolite water content by storing samples overnight in a controlled humidity container (RH 53%).

2.2. XRPD data collection

To evaluate if the type of instrumentation, the applied radiation and the sample loading method has any significant effect on the refined weight fractions, XRPD patterns were recorded on two different X-ray diffraction devices. A comparison was made between data collected in typical laboratory conditions and data recorded at the BM01b beam lime for high resolution powder diffraction at the European Synchrotron Radiation Facility (ESRF) in Grenoble, France.

Laboratory measurements were carried out at the department of Earth and Environmental Sciences at the K.U.Leuven on a Phillips PW1830 device with CuK$\alpha_{1,2}$ radiation at 30 mA and 45 kV using a graphite monochromator and a gas proportional scintillation detector. The samples were back loaded into the sample holders and horizontally spun during measurement to improve particle statistics. Diffractometer scans were recorded in Bragg-Brentano geometry from 5 to 70 º2θ, with a step size of 0.02 º2θ and 2 s counting time per step.

Synchrotron based data collection was performed with a wavelength of 0.49725 Å, calibrated against standard Silicon NIST SRM 640b. Samples were loaded into 2 mm glass capillaries and spun during measurement. XRPD patterns were collected in transmission mode over an angular range of 1-26.5 °2θ with a step size of 0.003 °2θ and a scan time per step of 200 ms. The resulting patterns consisted of the integrated and normalized intensity of six separate counting chains, mounted with an angular offset of 1.1 °2θ.

2.3. Rietveld refinement

The phase quantification procedure involved the identification of major and minor phases using the DiffracPlus EVA software (Bruker) and a subsequent quantitative phase analysis of all data sets by the full profile Rietveld method implemented in the Topas Academic v4.1 software (Coelho, 2007). Best result reproducibility was obtained when the complete 2θ ranges starting at *d*-value 14 Å were included in the refinement. A fundamental parameters approach was employed for the separate calculation of the instrumental and sample inherent contributions to the X-ray diffraction peak profiles (Cheary & Coelho, 1992). The starting structure models were adopted from literature, isotropic temperature factors were introduced in all models. In the initial refinement cycles global parameters, i.e. the overall zero error and phase scale factors, were refined. The background was fitted to a Chebyshev function of a gradually increased number of polynomial coefficients until a level of 15 terms was reached. Cell parameters and phase specific Lorentzian functions allowing for peak shape broadening were refined within constrained limits determined by bond distance requirements (Shannon & Prewitt, 1970). Cell parameters of the pure ZnO internal standard were calibrated against rutile NIST SRM 674 on a separate mixture and were fixed to the calibrated values during subsequent quantitative phase analysis.

In a next step, partial structure refinements of the main zeolite phases were undertaken. Structure refinements could only be performed on data sets where diffraction peak overlap was limited. Strong overlapping of mordenite and clinoptilolite reflection lines in samples D and F rendered structure refinement therefore impossible. The XRPD patterns collected at BM01b displayed significantly increased resolution. Therefore these data sets were selected as a basis for structural refinement of the remaining samples. The optimized structures were then introduced unchanged into the input files for quantitative phase analysis for both synchrotron and laboratory collected data sets. In the structure refinements, the atomic coordinates and atomic site occupancies of the extraframework cations and water molecules were refined in alternate cycles. The extraframework site occupancies and coordination were compared to literature data.

A local analysis of parameter sensitivity of Rietveld quantitative mineralogical analysis was performed. The dependence of the weight fractions of the zeolite phases and in particular the amorphous phase on discrete variations in fixed input parameters was evaluated. The selected input parameters for variation were the isotropic thermal factors of the ZnO internal standard and the number of refined background coefficients. The response of the refinement output to the input variation aids to clarify the significance of parameter uncertainties on the quantification outcome. Furthermore, it allows deriving sensible parameter constraints in order to obtain useful and precise refinement results. Additionally, differences between quantification results of different data sets were compared with estimated statistical standard deviations, further abbreviated as esd, as calculated from the least-squares refinement (Scott, 1983; Bérar & Lelann, 1991; Toraya, 2000).

3. Results and discussion

3.1 Structure refinement

The structure refinements started from structure models published in the literature (clinoptilolite: Snellings *et al.*, 2009; mordenite: Mortier *et al.*, 1976) and are separately reported as electronic supplementary data. The most remarkable differences of the refined structures with the literature models were situated in the site occupancies of the extraframework cations and water molecules. In the clinoptilolite refinements of samples A and C, a conspicuous rise was observed in the occupancy of sites where bivalent cations (Ca^{2+}; Mg^{2+}) enter preferentially

Table 2. Comparison between quantitative analysis results obtained before and after structure refinement. Only the phase abundances and esd's , in parentheses, calculated from the synchrotron data are tabulated. A significant improvement in the agreement indices is observed, however this does not reflect in significant changes in the calculated weight fractions of the zeolites or amorphous phase. The zeolite structures in samples D and F could not be refined due to excessive peak overlap of the mordenite and clinoptilolite zeolite phases.

	Before structure refinement				After structure refinement				Zeolite		Amorphous phase	
	Zeolite wt%	Amorphous phase wt%	R_{wp}	S	Zeolite wt%	Amorphous phase wt%	R_{wp}	S	Δrelative	Δabsolute	Δrelative	Δabsolute
A	71.2 (6)	7.4 (10)	17.7	1.23	71.7 (3)	6.6 (8)	17.4	1.21	0.7	-0.5	7.5	0.8
B	70.3 (2)	26.8 (9)	19.5	1.32	69.8 (1)	30.2 (9)	19.1	1.30	0.7	0.5	13.5	-1
C	93.3 (1)	4.6 (11)	19.2	1.30	93.4 (1)	5.2 (12)	18.9	1.27	0.1	-0.1	8.3	-0.6
D	47.9 (4)	20.7 (8)	15.1	1.25								
E	72.7 (1)	26.8 (9)	19.5	1.40	72.6 (1)	26.9 (9)	18.6	1.34	0.1	0.1	0.2	-0.1
F	55.3 (7)	43.6 (10)	19.4	1.33								
G	52.3 (4)	34.9 (9)	18.7	1.38	52.4 (4)	33.6 (9)	18.1	1.34	0.2	-0.1	2.5	1.3
Average									0.4	0	6.4	0.1

(M2 and M4, *cf*. Armbruster & Gunter, 2001). Changes in water content in all refined clinoptilolites and in site occupancies in sample B with respect to the initial structure model were less pronounced. It is not unequivocally possible to relate the bulk chemistry to the zeolite chemistry due to the presence of a considerable amorphous phase fraction of unknown composition and heterogeneity.

The mordenite refinements showed lower M1 site occupancies than those reported for the Ca-exchanged mordenite literature model. The presence of cations possessing fewer electrons such as Na^+ and K^+ can explain the reduced electron density encountered at the extraframework cation site. The presence of monovalent cations present in the mordenite channels also explains the lower calculated water contents in samples E and G.

In order to study the influence of the structure model on the quantitative phase analysis the results for the data collected at BM01b are given in Table 2, conjointly with the R_{wp} and S agreement indices. Fig. 1 presents an illustration of the experimentally collected and Rietveld calculated profiles of sample A after clinoptilolite structure refinement. It was observed that though the fit of the calculated pattern was significantly improved, the variations in zeolite phase abundances were negligible and did not exceed the esd values. This observation learns that the selected clinoptilolite and mordenite literature models initially fitted relatively well to the clinoptilolite reflections in the diffraction patterns and that the quantitative phase analysis results were in consequence relatively insensitive to the structure refinements. The amorphous phase content was found to be considerably more sensitive, yielding relative deviations of 0.2 to 13.5% and absolute deviations of -0.6 to 1.3%. The larger deviations in samples containing less amorphous phase originate partly from the lower levels of amorphous phase present and partly from the indirect calculation of the amorphous content from the refined amount of internal

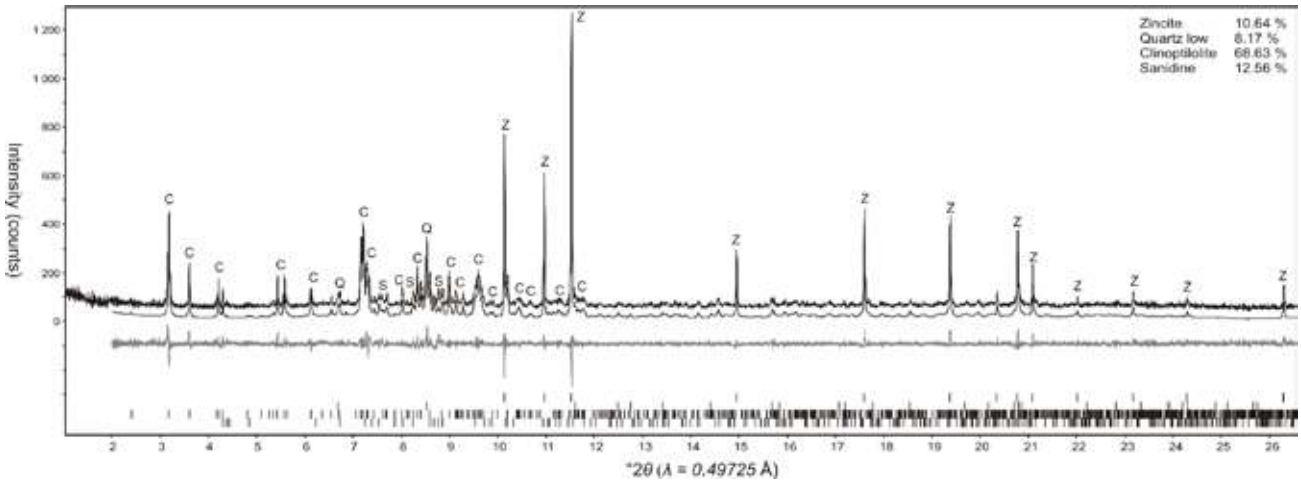

Figure 1. Rietveld refinement of sample A collected at BM01b (ESRF), 10 wt% ZnO was added as internal standard. The structure of clinoptilolite was refined. Above, the measured (broken line) and calculated pattern (full line) are presented, underneath the difference curve is given. Below, the reflection positions of the phases given in the upper right corner are displayed. C identifies with clinoptilolite, Q with quartz, S with sanidine (K-feldspar) and Z with zincite.

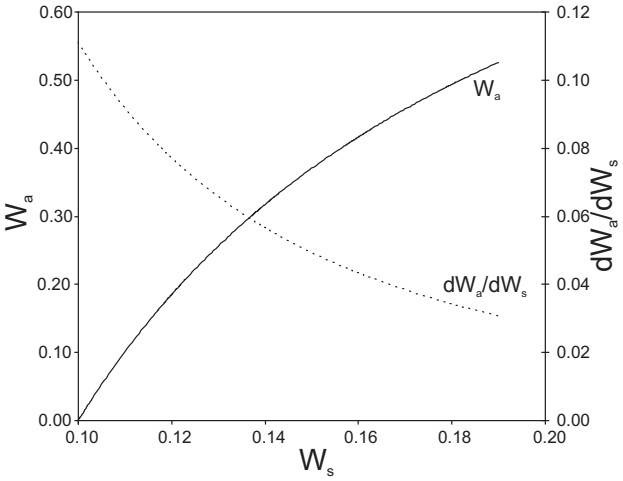

Figure 2. The calculated amorphous phase fraction (W_a) and its derivative (dW_a/dW_s), the local sensitivity, in function of the refined internal standard weight fraction (W_s), when 10 wt% of internal standard is added to the sample material.

standard. Additionally, both factors reinforce each other. Fig. 2 depicts the relationship between the amount of internal standard refined and the calculated amorphous phase content if a 10 wt% internal standard is added to the mixture. This relationship is mathematically expressed as in equation (5)

$$W_a = \left(1 - W_{s,w}\right)^{-1} \left(1 - \left(W_{s,w} / W_s\right)\right), \quad (5)$$

differentiating equation (6) with respect to W_s gives

$$dW_a / dW_s = \left(1 - W_{s,w}\right)^{-1} \left(W_{s,w} / W_s{}^2\right). \quad (6)$$

Equation (6) relates an infinitesimal variation in refined internal standard weight fraction with a corresponding change in amorphous weight fraction and can be used to evaluate the sensitivity of Rietveld quantitative amorphous content analysis when taking the internal standard approach. The corresponding function is displayed in Fig. 2 for an addition of 10 wt% internal standard. From this equation it is expected that relative and absolute uncertainties in amorphous phase fraction are largest when smaller amounts of amorphous phase are present in the samples, corroborating our observations.

3.2 Internal standard thermal parameters

One of the requirements of the internal standard is that it should have a simple known structure of high symmetry to avoid excessive complexity and overlap of peaks (Snyder & Bish, 1989). The details of the refined and calibrated ZnO structure model employed here are reported in Table 3 (structure adapted from Abrahams & Bernstein, 1969). The isotropic atomic temperature factors (B_{iso}) are included in the calculation of the structure factors *F(hkl)* and thus *I(hkl)* as follows (Giacovazzo *et al.*, 2002):

$$F(hkl) = \sum s_n o_n \exp\left(2\pi i \left(hx + ky + lz\right)\right) \exp\left(-B_{iso,n} \sin^2\theta / \lambda^2\right) \quad (7)$$

where s_n and o_n are the scattering factor and the site occupancy of an atom n in the unit cell respectively, *h, k, l* are the reflection indices, *x, y, z* are the atom fractional coordinates, θ is the diffraction angle and λ is the diffraction wavelength. It is then obvious that the atomic thermal parameters exert an important influence on the scale factors and the weight fractions. When the ZnO B_{iso} values were refined to the data collected at the synchrotron an important deviation from the values reported in the literature was observed, i.e. an overall value of 0.15 Å^2 or less was refined instead of 0.65 Å^2. This resulted in an important decrease of the calculated amorphous content. A similar refinement of ZnO B_{iso} of the laboratory data resulted in increased overall B_{iso} values varying from 0.7 to 1.2 Å^2, resulting in important increases in the calculated amorphous content. To clarify whether a refinement of the B_{iso} values is justified, constant overall thermal factors varying between an excessively small value of 0.06 Å^2 and an excessively large value of 6.00 Å^2 were applied to the ZnO and the effect on the calculated amorphous weight fraction was evaluated. Fig. 3 portrays the results for the refinements on synchrotron and laboratory data. The weight fraction data are expressed as a ratio of the calculated amount of amorphous phase at a specifically imposed ZnO B_{iso} ($W_{a,Biso}$) over the amount calculated at an imposed ZnO B_{iso} of 6.00 Å^2 ($W_{a,Biso=6}$). Changes in the ZnO B_{iso} result in large variations in the calculated amounts of amorphous phase. Most sensitive are samples A and C containing the lowest amorphous phase content (cf. section 3.1). It is apparent from Fig. 3a that a very shallow minimum in the curve of the R_{wp} indices is present around 0.15 Å^2 or less. This is associated with large uncertainties in the esd's (large residual shifts in the least squares minimization routine) of the ZnO B_{iso} values and in consequence also of the ZnO phase abundances. The behaviour of the R_{wp} curve resulting from the laboratory data refinements in Fig. 3c shows a somewhat deeper minimum around 1.00 Å^2. This difference in refined ZnO B_{iso} values is not expected as both measurements were carried out at room temperature. Owing to the high sensitivities and associated uncertainties of the amorphous phase fractions to variations in the isotropic thermal parameters of the internal standard, it is not thought advisable to refine the B_{iso} values. The repeatability of measurements on different equipment types is considerably biased by a refinement of the B_{iso} values.

Table 3. Internal standard zincite crystal structure information calibrated to rutile NIST SRM 674.

Zincite: $P6_3mc$; a = 3.25005 (2), c = 5.20665 (3)					
Site	*x*	*y*	*z*	*Occupancy*	B_{iso}
Zn	1/3	2/3	0	1.00	0.63
O	1/3	2/3	0.3825 (14)	1.00	0.68

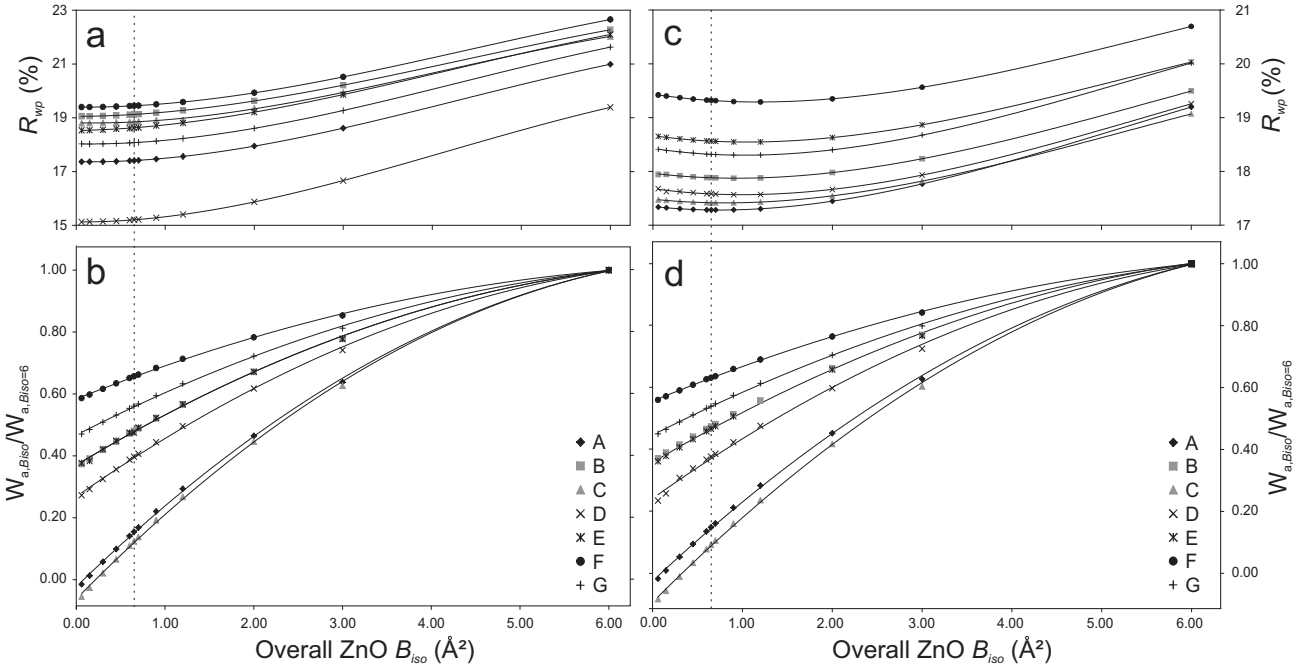

Figure 3. The variation of amorphous phase weight fractions in function of the imposed overall ZnO internal standard thermal factors (B_{iso}) for the synchrotron X-ray diffraction data (a and b) and the laboratory X-ray diffraction data (c and d). The variation is displayed in terms of R_{wp} agreement indices (a and c), and relative refined amorphous weight fraction with respect to the amount of amorphous phase calculated for overall ZnO B_{iso} of 6.00 Å² (b and d). The dashed line represents the ZnO thermal factors as given in Table 3.

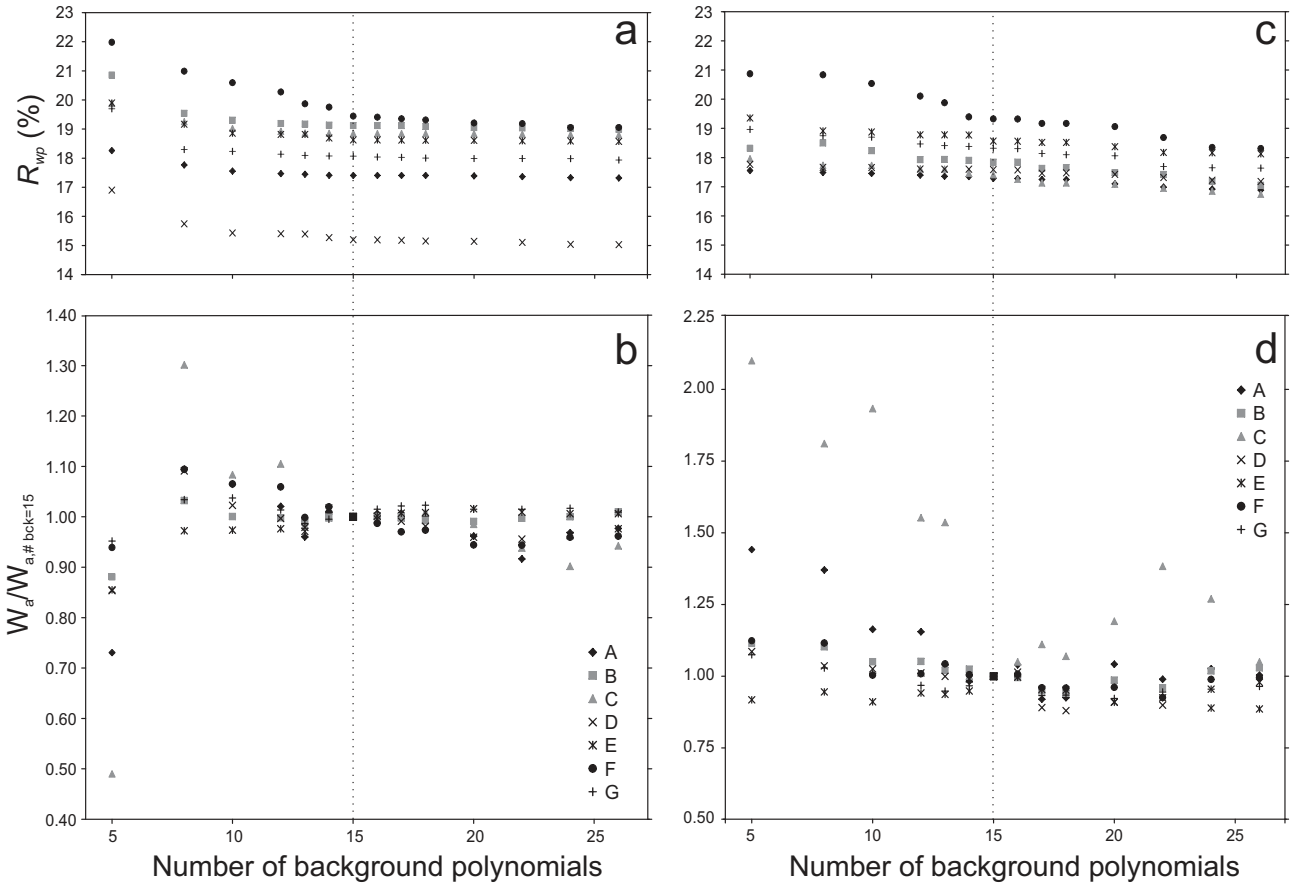

Figure 4. The variation of amorphous phase weight fractions in function of the imposed number of Chebyshev background polynomials for the synchrotron data (a-b) and the laboratory data (c-d). The variation is displayed in terms of R_{wp} agreement indices (a and c), and relative refined amorphous weight fraction with respect to the amount of amorphous phase calculated for 15 refinable terms in the Chebyshev function (b and d).

3.3 Background coefficients

In powder diffraction analyses the observed background signal arises from incoherent and diffuse X-ray scattering. Incoherent scattering arising from thermal motion of atoms, lattice defects and disorder in crystals is accounted for by the refinement of peak profile function parameters. Other contributions originating from air and sample holder scattering, Compton scattering, and diffuse scattering in imperfect crystals and amorphous phases are usually fitted by empirical higher order polynomial functions (Richardson, 1993; Larson & Von Dreele, 2004). The background intensity was calculated by a 'Chebyshev polynomial of the first kind' implemented in the Topas Academic software as:

$$I_b(2\theta) = \sum_{j=1}^{N} B_j T_{j-1}(2\theta) \quad (8)$$

where N is the selected highest order of the Chebyshev polynomials, B_j are refined weighting parameters, and T_j are the Chebyshev polynomials of order j.

Previous research indicated that an over- or underestimation of the polynomial order could result in a significant lowering of the accuracy of the amorphous phase fraction estimate. For a synthetic mixture with known amorphous phase content, Gualtieri (2000) reported that the background function should consist of at least 15 polynomial terms to achieve an accurate estimate. Less terms induced an underestimation of the background contribution and a consequential overestimate of the amorphous fraction. Introducing larger numbers of background terms increased parameter correlation, but seemed to result in less deviant results. Here, we describe the extension of these results to more complex natural samples. The influence of the polynomial order on the amorphous phase fraction estimate was determined by varying the number of Chebyshev polynomials in a range from 5 to 26 and refining the weighting parameters. For both the synchrotron and laboratory collected data sets, the variation of the amorphous phase fraction relative to the reference of 15 polynomials is graphically displayed in Fig. 4 (b and d), conjointly with the corresponding R_{wp} agreement indices (a and c). An increase of the number of background polynomials from 5 to 13-14 was observed to improve the fit. Additionally, relative variations of the amorphous phase fraction significantly declined when the number of refinable parameters was raised. In the polynomial order range of 13 to 20 the amorphous fraction results remained relatively constant. Only when the orders were raised above 20, a majority of samples showed a sudden small fit improvement and corresponding deviations of phase fractions from the reference. A closer examination indicated that the N> 20 polynomial background curves improperly compensated misfits between the calculated and observed peak intensities at low angles (Fig. 5). It is apparent that the laboratory data are much more sensitive to variations in the number of background polynomials than the synchrotron data. The synchrotron data benefit strongly from the increased signal to noise ratio and resolution, resulting in a better resolved and thus more stably numerically modelled background. Samples with the smallest amorphous fraction obviously presented the largest sensitivity.

3.4 Data collection strategies

Data collection at the synchrotron BM01b beam line for high-resolution powder diffraction offered the advantages of a greatly enhanced intensity and brilliance of the monochromatic beam combined with modern multichannel detector systems. Compared to a traditional CuK$\alpha_{1,2}$ laboratory radiation source equipped with a gas proportional scintillation detector, this allowed for far better counting statistics, peak resolution and peak-to-background discrimination even when employing much shorter data collection times. Fig. 6 depicts both diffraction patterns for sample C. It is observed that the contribution of the instrument on peak profile broadening is drastically reduced in the synchrotron collected data, moreover signal integration over six separate counting chains led to an obvious improvement of the signal to background ratio. The apparent noise on the synchrotron signal is mainly

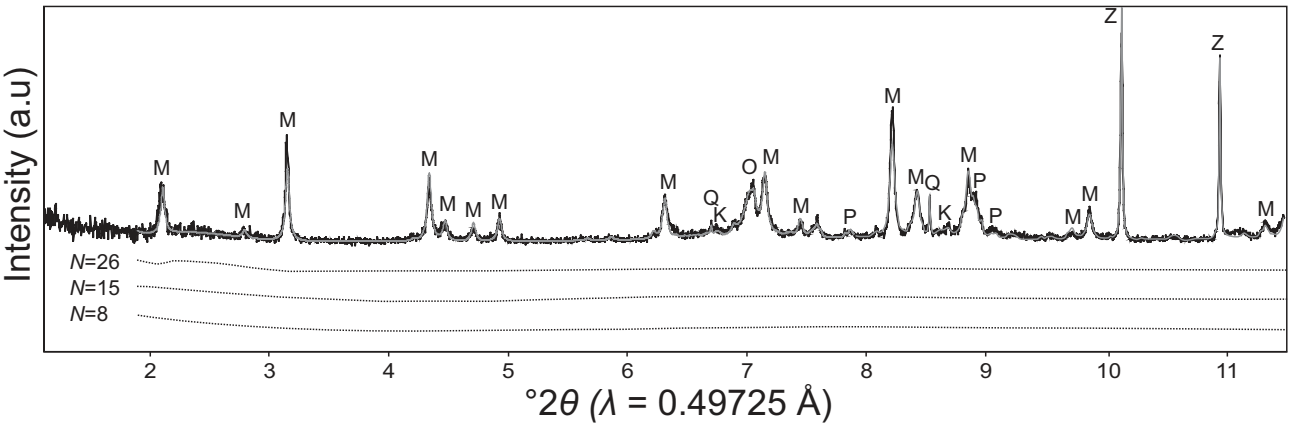

Figure 5. Selected 1-11.5° 2θ range of the diffraction pattern of sample G collected at BM01b.The refined background curves for a Chebyshev function of the 8th, 15th and 26th order are plotted (M = mordenite, Q = quartz, K, = K-feldspar, P = plagioclase, Z = zincite)

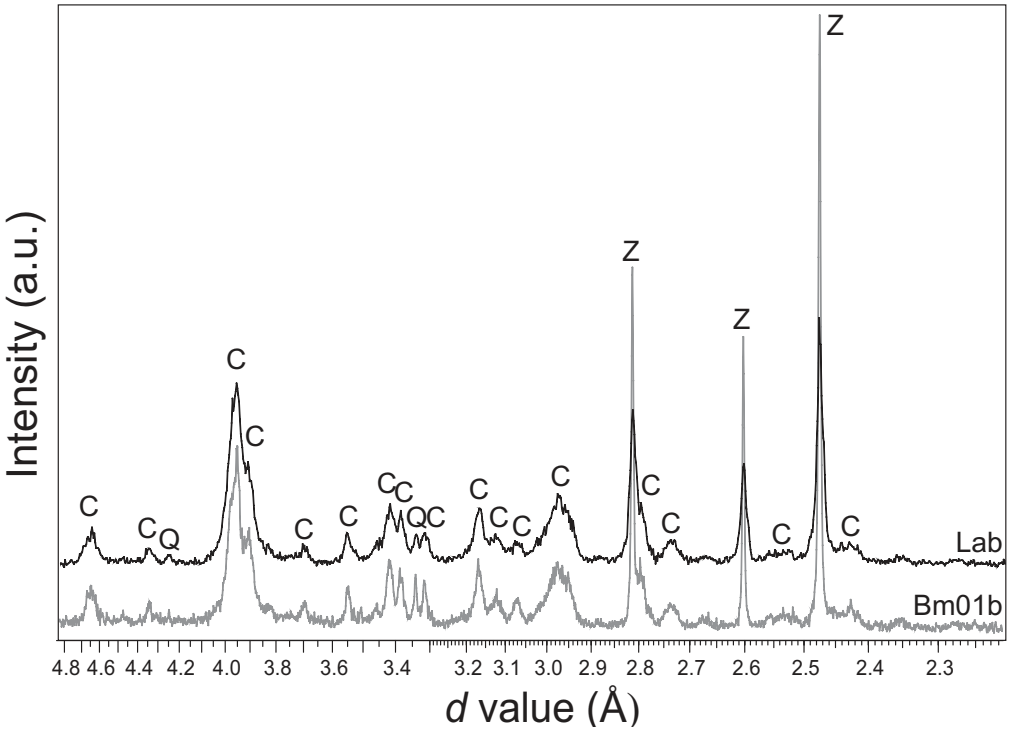

Figure 6. Comparison between the laboratory and BM01b X-ray diffraction patterns of sample C over the range of 4.8 to 2.2 Å (C = clinoptilolite, Q = quartz, Z = zincite).

due to the much smaller scanning step size. The improved peak resolution and counting statistics allowed for more stable and reliable structure refinements departing from the BM01b beam line data.

The zeolite and amorphous phase quantitative mineralogical results obtained by refinement of both data sets are plotted with respect to each other in Fig. 7. All values plot close to the 1:1 ratio bisector, implying that the reproducibility of the analyses is very good. The largest esd values were calculated for the amorphous phase fractions. Invariably the esd values obtained from the laboratory experiments were larger relative to the synchrotron esd values due to worse counting statistics. The good reproducibility of the phase fraction estimates indicates that equivalent quantitative mineralogical analysis results can be obtained from laboratory equipment if a careful analysis is carried out. Similarly, Madsen *et al*. (2001) reported that the accuracy of the results is more strongly biased by the operator experience than by the equipment used for data collection.

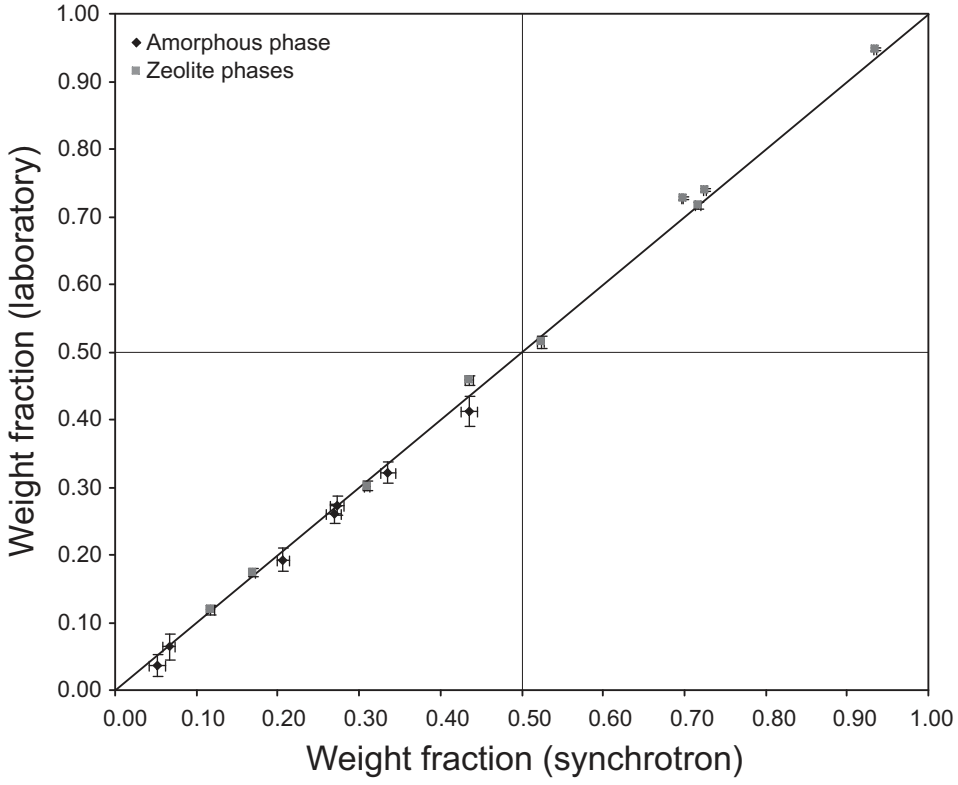

Figure 7. Correlation plot of the weight fractions refined from the corresponding BM01b and laboratory collected diffraction patterns. The weight fractions of zeolite and amorphous phases are given with their respective esd's. The number of refinable background coefficients was 15, constant literature ZnO thermal parameters were used, no preferred orientation correction was applied.

Preferred orientation effects are commonly encountered when measuring on flat plate sample holders, especially in minerals showing a preferential basal cleavage. The effects of preferred orientation can be alleviated by appropriate sample preparation. Measurement in spinning capillaries is generally considered as being most effective in removing preferred orientation effects, though minerals with an elongated rod-like morphology can be oriented along the capillary axis (McCusker *et al.*, 1999; Madsen *et al.*, 2001). The mordenite crystal habit is fibrous, often showing fine needles elongated along the *c*-axis. Clinoptilolite crystallizes as coffin shaped platelets with a basal cleavage plane along (020) (Armbruster & Gunter, 2001). Preferred orientation can thus be expected to be present in both flat-plate (clinoptilolite) and capillary (mordenite) loaded samples. Several of the observed clinoptilolite and mordenite reflection intensities indeed deviated sufficiently from the calculated intensities to suspect preferred orientation. The refinement of preferred orientation modeling parameters for the zeolite phases in the March-Dollase model (Dollase, 1986) or using spherical harmonics (Ahtee *et al.*, 1989; Von Dreele, 1997) of varying harmonic order between 2 and 8 generally improved the fit between calculated and observed patterns. However, the reproducibility of the phase fraction results was strongly exacerbated. In Fig. 8 a comparison is made between the quantification results obtained from corresponding BM01b and laboratory collected diffraction profiles when preferred orientation corrections are introduced. The agreement between the amorphous phase quantification outcomes of the synchrotron and laboratory measurements is considerably worsened by applying increasingly 'powerful' preferred orientation corrections for the zeolite phases. The amount of scatter increases considerably and the R^2 (squared Pearson product moment) correlation coefficients decrease when applying higher spherical harmonic order corrections. It was apparent that the correction factors overly compensated for pattern misfits that were not realistically attributable to preferred orientation. This leads to systematic errors and prevents an accurate assessment of the abundances of structurally variable phases such as zeolites or clays (De La Torre *et al.*, 2001). The influence of preferred orientation on scale factors of phases showing large numbers of reflections are expected to be effectively minimized by Rietveld full profile fitting (Snyder & Bish, 1989).

4. Conclusions

The refinement strategy for quantitative mineralogical analysis in zeolitized tuffaceous rocks containing clinoptilolite and mordenite is critically assessed by local sensitivity analyses of selected important parameters in the Rietveld refinement method. Though limited to a particular type of geological material, the findings carry broader implications and guidelines for quantitative mineralogical analysis using the Rietveld method on X-ray powder diffraction patterns.

Zeolite species generally show a large crystal chemical variability. In consequence calculated structure models and reflection intensities do not necessarily match observed diffraction patterns. However, refinement of the

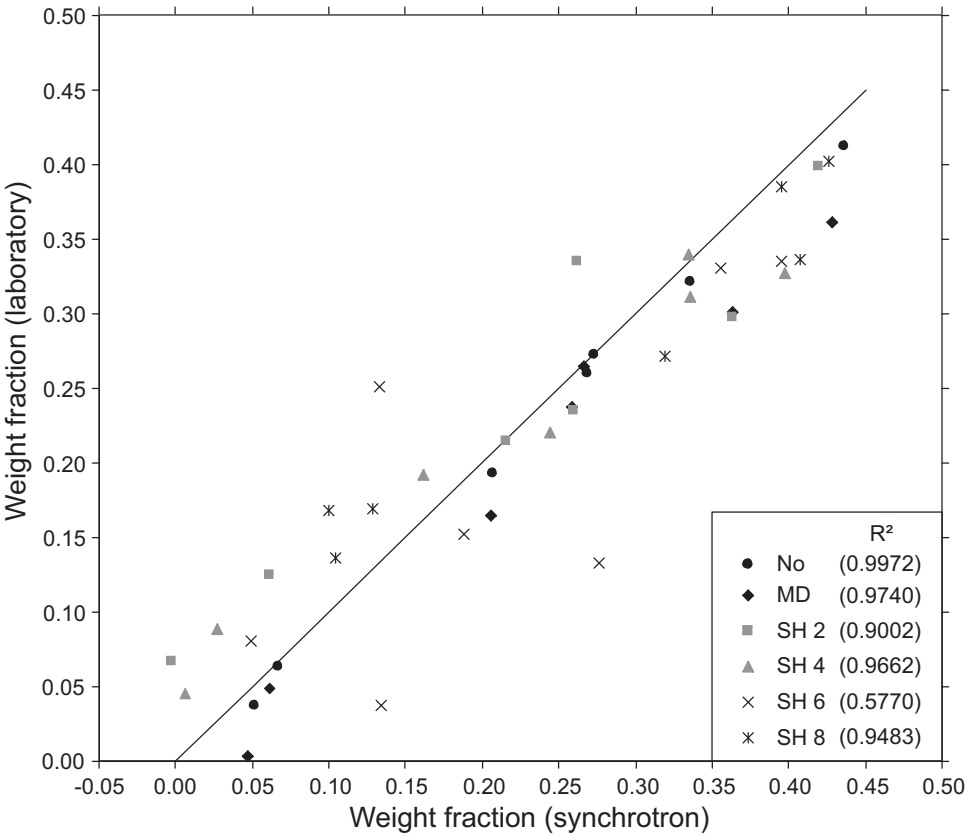

Figure 8. Correlation plot showing the results of introducing preferred orientation corrections upon the weight fractions refined from the corresponding BM01b and laboratory collected diffraction patterns. The preferred orientation corrections considered range from March-Dollase corrections (MD) for specified groups of reflection along a specific direction (i.e. (020) for clinoptilolite and (200) for mordenite) to spherical harmonics corrections (SH) of harmonic order varying from 2 to 8. For comparison the quantification results without preferred orientation correction (No) are displayed. Between brackets the R^2 (i.e. the squared Pearson product moment) correlation coefficients are given. The number of refinable background coefficients was 15 and constant literature ZnO thermal parameters were used in the refinement.

investigated zeolite structures did not effectuate important changes in the estimated phase contents if appropriate literature models were selected.

When using the internal standard approach, the calculated amorphous phase fraction was shown to be very sensitive to the amount of refined internal standard, especially when low amounts of amorphous phase were present in the samples. Therefore, the actual weight ratio of the internal standard over the sample material in the measured mixture should be accurately determined. In the case of zeolites, which show a reversible hydration behaviour, the samples should be stored in a controlled humidity environment.

The refined amorphous content was very sensitive to the refinement of the isotropic thermal parameters of the employed ZnO internal standard. This resulted in very large uncertainties in the calculation procedure and deteriorated reproducibility of the analyses. Therefore, appropriate literature structure models should be chosen for the employed internal standard.

In samples containing a significant amount of amorphous material incoherent and diffuse scattering gives rise to an increased background signal. A sufficient number of background polynomials and refinable weighting factors should be employed to numerically approximate the background. The samples under consideration showed optimal repeatability in the range of 13 to 20 polynomials. Introducing more polynomials resulted in incorrect parameter correlations.

The good reproducibility of the phase abundance results by synchrotron and laboratory based powder diffraction systems, often within one esd, corroborate the use of laboratory equipment for quantitative mineralogical analysis. The demonstrated dependence of phase fraction calculations on refinement inherent parameter choices, learns that cautious refinement strategies and operator experience should be considered to be more important factors than type of instrumentation in quantitative phase analysis by Rietveld refinement. Preferred orientation corrections were observed to have an adverse effect on the reproducibility of the results, and were therefore avoided in the refinement.

5. Acknowledgements

The authors wish to thank the European Synchrotron Radiation Facility for the provision of beam time. Wouter Van Beek is gratefully acknowledged for the experimental assistance at the Swiss-Norwegian beam line (BM01b). The reviews of Dr Giovanni Ferraris, Dr Tobias Weisenberger and an anonymous referee were highly appreciated and significantly improved the paper quality. Ruben Snellings is currently working as Aspirant of the Research Foundation – Flanders (FWO).

6. References

Suplementary data for this paper are available at Geologica Belgica on line.

ABRAHAMS, S.C. & BERNSTEIN, J.L., 1969. Remeasurement of the structure of hexagonal ZnO. *Acta Crystallographica B.,* 25: 1233-1236.

AHTEE, M., NURMELA, M., SUORTTI, P. & JÄRVINEN, M., 1989. Correction for preferred orientation in Rietveld refinement. *Journal of Applied Crystallography,* 22: 261-268.

ARMBRUSTER, T. & GUNTER, M.E., 2001. Crystal structures of natural zeolites. *In:* Bish, D.L. & Ming, D.W., *Natural zeolites: occurrence, properties, applications*. Reviews in mineralogy and geochemistry, Mineralogical Society of America, Washington DC, 45: 1-68.

BARKER, J.M., FREEMAN, P.S., AUSTIN, G.S., BOWMAN, R.S., 2004. Development of value-added zeolite products from St. Cloud Mining. *CIM Bulletin*, 97: 1-7.

BENITO, R., GARCIA-GUINEA, J., VALLE-FUENTES, F.J., RECIO, P., 1998. Mineralogy, geochemistry and uses of the mordenite–bentonite ash-tuff beds of Los Escullos, Almería, Spain. *Journal of Geochemical Exploration*, 62: 229-240.

BÉRAR, J. -F. & LELANN, P., 1991. E.S.D's and estimated probable error obtained in Rietveld refinements with local correlations. *Journal of Applied Crystallography,* 24: 1-5.

BISH, D. & HOWARD, S.A., 1988. Quantitative phase analysis using the Rietveld method. *Journal of Applied Crystallography*, 21, 86-91.

BISH, D.L. & POST, J.E, 1993. Quantitative mineralogical analysis using the Rietveld full-pattern fitting method. *American Mineralogist,* 78:932-940.

BRINDLEY, G.W., 1945. The effect of grain or particle size on X-ray reflections from mixed powders and alloys, considered in relation to the quantitative determination of crystalline substances by X-ray methods. *Philosophical Magazine (Series 7),* 36, 347-369.

CHEARY, R.W., COELHO, A.A., 1992. A fundamental parameters approach of X-ray line-profile fitting. *Journal of Applied Crystallography,* 25: 109-121.

COELHO, A.A., 2007. Topas Academic v4.1, http://members.optusnet.com.au/~alancoelho/.

DE LA TORRE, A.G., BRUQUE, S. & ARANDA, M.A.G., 2001. Rietveld quantitative amorphous content analysis. *Journal of Applied Crystallography,* 34: 196-202.

DOLLASE, W.A., 1986. Correction of intensities for preferred orientation in powder diffractometry: Application of the March Model. *Journal of Applied Crystallography,* 19: 267-272.

EBERL, D.D., 2003. *User guide to RockJock, a program for determining quantitative mineralogy from powder X-ray diffraction data*. USGS Open File Report OF 03-78, 40 pp.

EYDE, T.H., 1982. Zeolite deposits in the Gilda and San Simon valleys of Arizona and New Mexico. New Mexico *Bureau of Mines & Mineral Resources,* 182: 65-71.

FLOOD, P.G., TAYLOR, J.C., 1991. Mineralogy and geochemistry of Late Carboniferous zeolites, near Werris Creek, New South Wales, Australia. *Neues Jahrbuch für Mineralogie-Monatshefte,* 2: 49-62.

GIACOVAZZO, C., MONACO, H.L., VITERBO, D., SCORDARI, F., GILLI, G., ZANOTTI, G. & CATTI, M., 2002. *Fundamentals of Crystallography.* IUCr texts on Crystallography, 7, Oxford University Press, 825 pp.

GUALTIERI, A., 1996. Modal analysis of pyroclastic rocks by combined Rietveld and RIR methods. *Powder diffraction,* 11: 97-106.

GUALTIERI, A.F. & BRIGNOLI, G., 2004. Rapid and accurate quantitative phase analysis using a fast detector. *Journal of Applied Crystallography,* 37: 8-13.

GUALTIERI, A.F., 2000. Accuracy of XRPD QPA using the combined Rietveld-RIR method. *Journal of Applied Crystallography*, 33: 267-278.

GUALTIERI, A.F., VIANI, A. & MONTANARI, C., 2006. Quantitative phase analysis of hydraulic limes using the Rietveld method. *Cement and Concrete Research,* 36: 401-406.

GUDE, A.J. & SHEPPARD, R.A., 1988. A zeolitic tuff in a lacustrine facies of the Gila Conglomerate near Buckhorn, Grant County, New Mexico. *Bulletin of the US Geological Survey,* 1763, 22 p.

HILL, R.J. & HOWARD, C.J, 1987. Quantitative phase analysis from neutron powder diffraction data using the Rietveld method. *Journal of Applied Crystallography,* 20: 467-474.

HILL, R.J., 1991. Expanded use of the Rietveld method in studies of phase abundance in multiphase mixtures. *Powder Diffraction,* 6: 74-77.

HONRADO, M.L., PASCUA, C.S., VARGAS, E., ARCILLA, C.A., ALEXANDER, W.R., NAMIKI, K., FUJII, N., YAMAKAWA, M., SATO, T., MCKINLEY, I.G., 2009. Smectite and zeolite formation from the pyroclastic deposits of the Aksitero Formation, Philippines. *Geochimica et Cosmochimica Acta*, 73, Supplement 1: A547.

KLUG, H.P. & ALEXANDER, L.E., 1974. *X-ray powder diffraction procedures for polycrystalline and amorphous materials*. Wiley, New York, 992 pp.

LARSON, A.C &, VON DREELE, R.B., 2004. *General Structure Analysis System (GSAS),* Los Alamos National Laboratory Report LAUR 86-748.

MADSEN, I.C., SCARLETT, N.V.Y., CRANSWICK, L.M.D. & LWIN, T., 2001. Outcomes of the International Union of Crystallography commission on powder diffraction round robin on quantitative phase analysis: samples 1a to 1h. *Journal of Applied Crystallography,* 34: 409-426.

McCUSKER, L.B., VON DREELE, R.B., COX, D.E., LOUËR, D. & SCARDI, P., 1999. Rietveld refinement guidelines. *Journal of Applied Crystallography,* 32: 36-50.

MITCHELL, L.D., MARGESON, J.C. & WHITFIELD, P.S., 2006. Quantitative Rietveld analysis of hydrated cementitious systems. *Powder Diffraction,* 21: 111-113.

MORTIER, W.J., PLUTH, J.J & SMITH, J.V., 1976. Positions of cations and molecules in zeolites with the mordenite-type framework, III. Rehydrated Ca-exchanged ptilolite. *Materials Research Bulletin,* 11: 15-22.

PRITULA, O., SMRČOK, L., TÖBBENS, D.M. & LANGER, V., 2004. X-ray and neutron Rietveld quantitative phase analysis of industrial Portland cement clinkers. *Powder Diffraction*, 19: 232-238.

RICHARDSON, J.W., 1993. Background modelling in Rietveld analysis. *In:* R.A. Young (Ed.) *The Rietveld Method*. IUCr Monographs on Crystallography 5, Oxford University Press, 102-109.

RIETVELD, H.M., 1969. A profile refinement method for nuclear and magnetic structures. *Journal of Applied Crystallography*, 2: 65-71.

SCARLETT, N.V.Y., MADSEN, I.C., MANIAS, C. & RETALLACK, D., 2001. On-line X-ray diffraction for quantitative phase analysis: Application in the Portland cement industry. *Powder Diffraction*, 16: 71-80

SCOTT, H.G., 1983. The estimation of standard deviations in powder diffraction Rietveld refinements. *Journal of Applied Crystallography*, 16: 159-163.

SHANNON, R.D. & PREWITT, C.T., 1970. Revised values of effective ionic radii. *Acta Crystallographica B*, 26: 1046-1048.

SNELLINGS, R.A., GUALTIERI, A.F. & ELSEN, J., 2009. The Rietveld refinement of an exceptionally pure sample of clinoptilolite from Ecuador and its Na-, K-, and Ca-exchanged forms. *Zeitschrift für Kristallographie Supplement*, 30: 395-400.

SNYDER, R.L. & BISH, D.L., 1989. Quantitative analysis. In Bish, D.L. & Post, J.E., eds. Reviews in Mineralogy, Modern powder diffraction. *Mineralogical Society of America*, 20: 101-144.

ŚRODOŃ, J., DRITS, V.A., McCARTY, D.K., HSIEH, J.C.C. & EBERL, D.D., 2001. Quantitative X-ray diffraction analysis of clay bearing rocks from random preparations. *Clays and Clay Minerals*, 49: 514-528.

SUHERMAN, P.M., VAN RIESSEN, A., O'CONNOR, B., LI, D., BOLTON, D. & FAIRHURST, H., 2002. Determination of amorphous levels in Portland cement clinker. *Powder Diffraction*, 17: 178-185.

TAYLOR, J.C. & MATSULIS, C.E., 1991. Absorption contrast effects in the quantitative XRD analysis of powders by full multiphase profile refinement. *Journal of Applied Crystallography*, 24: 14-17.

TORAYA. H., 2000. Estimation of statistical uncertainties in quantitative phase analysis using the Rietveld method and the whole-powder-pattern decomposition method. *Journal of Applied Crystallography,* 33: 1324-1328.

VON DREELE, R.B., 1997. Quantitative texture analysis by Rietveld refinement. *Journal of Applied Crystallography,* 30: 517-525.

WALENTA, G. & FÜLLMANN, T., 2004. Advances in quantitative XRD analysis for clinker, cements and cementitious additions. *Powder Diffraction*, 19: 40-44.

WEISENBERGER, T. & SPÜRGIN, S., 2009. Zeolites in alkaline rocks of the Kaiserstuhl Volcanic Complex, SW Germany - new microprobe investigation and the relationship of zeolite mineralogy to the host rock. *Geologica Belgica,* 12: 75-91.

YOUNG, R.A., 1993. *The Rietveld Method*. IUCr Monographs on Crystallography 5. Oxford University Press, 298 pp.

Manuscript received 24.09.2009, accepted in revised form 21.01.2010, available on line 15.02.2010